

Invariant form of spin-transfer switching condition

Inti Sodemann¹ and Ya. B. Bazaliy^{1,2,*}

¹*Department of Physics and Astronomy, University of South Carolina, Columbia, SC 29208, USA*

²*Institute of Magnetism, National Academy of Science, Kyiv 03142, Ukraine*

(Dated: June 24, 2009)

We derive an invariant form of the current-induced switching condition in spin-transfer devices and show that for energy minima and maxima the “switching ability” of the current is determined by the spin torque divergence. In contrast, energy saddle points are normally stabilized by current-induced merging with other equilibria. Our approach provides new predictions for several experimental setups and shows the limitations of some frequently used approximations.

High density electric currents induce magnetization motion and switching in nano-size metallic wires containing alternating ferromagnetic and non-magnetic layers (Fig. 1(a)). This phenomenon is finding important applications in computer memory and logic devices. Switching is caused by the spin-transfer torque τ_{st} ^{1,2} which depends on the current, spin polarization, material parameters and the geometry of the device. Once τ_{st} is found, the magnetization dynamics can be obtained from the Landau-Lifshitz-Gilbert (LLG) equation. A simple but often sufficiently accurate approximation is the macrospin model that assumes uniform magnetization of the layer $\mathbf{M}(r,t) = M\mathbf{n}(t)$, where M is the saturation magnetization value and \mathbf{n} is a unit vector. In this case the LLG equation reads

$$\dot{\mathbf{n}} = \left[-\frac{\partial \varepsilon}{\partial \mathbf{n}} \times \mathbf{n} \right] + \tau_{st}(\mathbf{n}) + \alpha[\mathbf{n} \times \dot{\mathbf{n}}], \quad (1)$$

where $\varepsilon(\mathbf{n}) = (\gamma/M)E(\mathbf{n})$, $E(\mathbf{n})$ is the magnetic energy per unit volume, γ is the gyromagnetic ratio, and α is the Gilbert damping constant. The spin-transfer torque is proportional to electric current, $\tau_{st} \sim I$. At $I = 0$ vector \mathbf{n} assumes an equilibrium position \mathbf{n}_{eq} at a minimum of magnetic energy. A nonzero current has two effects: First, the spin torque gradually shifts the equilibrium away from its original position $\mathbf{n}_{eq}(I = 0) \rightarrow \mathbf{n}_{eq}(I)$. Second, a stable equilibrium may abruptly turn unstable at a critical current I_c , causing magnetic switching.²

Computation of I_c for a given equilibrium is a straightforward though cumbersome mathematical procedure. It would be much simplified if one could find a single quantity that determines the “switching ability” of spin torque at a given equilibrium \mathbf{n}_{eq} . Often, it is implicitly assumed that the magnitude $|\tau_{st}(\mathbf{n}_{eq})|$ itself is the relevant quantity, and, in particular, a sharp difference should exist between the destabilization of “collinear” ($\tau_{st}(\mathbf{n}_{eq}) = 0$) and “non-collinear” ($\tau_{st}(\mathbf{n}_{eq}) \neq 0$) equilibria. This view is certainly oversimplified, and it was argued³ that the critical current should also depend on the derivatives of τ_{st} . Here we show that the “switching ability” can be indeed introduced for extremum (minimum or maximum) energy points and in some cases for energy saddle points, and find explicit expressions for it. We apply our approach to a number of experimental devices, obtain a new qualitative understanding of their dynamics, and clarify

the limitations of some approximations.

The LLG equation (1) can be equivalently written as

$$(1 + \alpha^2) \dot{\mathbf{n}} = \mathbf{F}(\mathbf{n}) \equiv \boldsymbol{\tau}(\mathbf{n}) + \alpha \mathbf{n} \times \boldsymbol{\tau}(\mathbf{n}), \quad (2)$$

with $\boldsymbol{\tau} = \boldsymbol{\tau}_c + \boldsymbol{\tau}_{st}$, $\boldsymbol{\tau}_c = -[(\partial \varepsilon / \partial \mathbf{n}) \times \mathbf{n}]$. The equilibrium magnetization orientations \mathbf{n}_{eq} satisfy $\boldsymbol{\tau}(\mathbf{n}_{eq}) = 0$. Their stability can be investigated by linearizing the equation of motion. In spherical coordinates (ϕ, θ) one decomposes $\mathbf{F} = F^\phi \mathbf{e}_\phi + F^\theta \mathbf{e}_\theta$ in terms of the unit vectors \mathbf{e}_ϕ , \mathbf{e}_θ along the coordinate lines and obtains:

$$\begin{pmatrix} \dot{\delta\phi} \\ \dot{\delta\theta} \end{pmatrix} = \begin{pmatrix} \frac{1}{\sin\theta} \frac{\partial F^\phi}{\partial\phi} & \frac{1}{\sin\theta} \frac{\partial F^\phi}{\partial\theta} \\ \frac{\partial F^\theta}{\partial\phi} & \frac{\partial F^\theta}{\partial\theta} \end{pmatrix} \begin{pmatrix} \delta\phi \\ \delta\theta \end{pmatrix} = \hat{D} \begin{pmatrix} \delta\phi \\ \delta\theta \end{pmatrix}. \quad (3)$$

Stability of an equilibrium requires both eigenvalues of the “dynamic matrix” \hat{D} to have negative real parts. This is equivalent to

$$\text{Tr} \hat{D}(\mathbf{n}_{eq}) < 0, \quad \det \hat{D}(\mathbf{n}_{eq}) > 0. \quad (4)$$

Noticing that matrix \hat{D} is not covariant, we are led to introduce the related matrix of covariant derivatives

$$\hat{D}_{cov} = \begin{pmatrix} \frac{1}{\sin\theta} \frac{\partial F^\phi}{\partial\phi} + \frac{\cos\theta}{\sin\theta} F^\theta & \frac{1}{\sin\theta} \frac{\partial F^\phi}{\partial\theta} \\ \frac{\partial F^\theta}{\partial\phi} - \cos\theta F^\phi & \frac{\partial F^\theta}{\partial\theta} \end{pmatrix}.$$

The trace of \hat{D}_{cov} is an invariant quantity equal to

$$\text{Tr} \hat{D}_{cov} = \text{div} \mathbf{F} = \frac{1}{\sin\theta} \left(\frac{\partial}{\partial\theta} (\sin\theta F^\theta) + \frac{\partial F^\phi}{\partial\phi} \right).$$

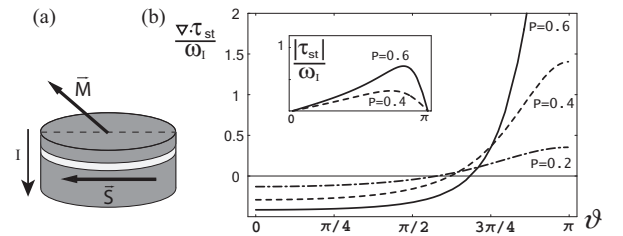


FIG. 1: (a) Typical spin-transfer device. (b) Angular dependence of the divergence and magnitude (inset) of the Slonczewski's spin torque term² for different polarizations P .

Crucially, $\hat{D} = \hat{D}_{cov}$ at equilibrium points. Hence, an invariant condition $\text{div}\mathbf{F} < 0$ can be used instead of the first inequality in (4). The latter is relevant for treating the equilibria corresponding to the energy extrema (minima and maxima). In this case $\det \hat{D}_{I=0} > 0$, with $\text{Tr} \hat{D}_{I=0} < 0$ at the minimum and $\text{Tr} \hat{D}_{I=0} > 0$ at the maximum points. Thus the condition of destabilization or stabilization is the change of sign of the trace, i.e., of $\text{div}\mathbf{F}$. Using the relation between \mathbf{F} and $\boldsymbol{\tau}$ and notation $\text{div}\mathbf{F} = \nabla \cdot \mathbf{F}$, where ∇ operates in the \mathbf{n} -space, we find:

$$\nabla \cdot \mathbf{F} = \nabla \cdot \boldsymbol{\tau} - \alpha [\nabla \times \boldsymbol{\tau}] \cdot \mathbf{n}, \quad (5)$$

where $[\nabla \times \boldsymbol{\tau}] \cdot \mathbf{n} = -(\partial\tau_\theta/\partial\phi - \partial(\sin\theta\tau_\phi)/\partial\theta)/\sin\theta$. The general expression for the spin-torque created by a polarizer pointing along the unit vector \mathbf{s} reads:

$$\boldsymbol{\tau}_{st}(\mathbf{n}, I) = \omega_I g(\mathbf{n} \cdot \mathbf{s}) [\mathbf{n} \times (\mathbf{s} \times \mathbf{n})] \equiv \omega_I \mathbf{f}_{st}(\mathbf{n}), \quad (6)$$

where $\omega_I = (\gamma/M)(\hbar I/2eV)$, V is the magnetic layer volume, e is the electron charge, and $g(\mathbf{n} \cdot \mathbf{s})$ is the efficiency factor.⁴ Using $\nabla \cdot \boldsymbol{\tau}_c = 0$ and $[\nabla \times \boldsymbol{\tau}_{st}] \cdot \mathbf{n} = 0$ we get

$$\nabla \cdot \mathbf{F} = \nabla \cdot \boldsymbol{\tau}_{st} - \alpha \nabla \times \boldsymbol{\tau}_c = \omega_I \nabla \cdot \mathbf{f}_{st} - \alpha \nabla^2 \varepsilon. \quad (7)$$

Here the first term is proportional to the current and can lead to the sign change of the whole expression. We see that the switching ability is determined by the divergence $\nabla \cdot \mathbf{f}_{st}$ that characterizes the angular dependence of the spin torque. Note that with Eq. (7) condition $\text{div}\mathbf{F} = 0$ can be viewed as a limiting case of the condition for the existence of a precession cycle (P), $\oint (\boldsymbol{\tau}_{st} \cdot \mathbf{e}_\perp) d\mathbf{l} = \alpha \oint ([\nabla \varepsilon \times \mathbf{n}] \cdot \mathbf{e}_\perp) d\mathbf{l}$, where integrals are taken along the cycle.⁵ In terms of the bifurcation theory,⁶ local destabilization of the minimum points is the *Hopf bifurcation* which normally produces a stable precession cycle.

Consider now the experimentally relevant case of small Gilbert damping, $\alpha \ll 1$. Expression (7) shows that the critical current satisfies $I_c \propto \alpha$ and hence will also be small. Therefore at $I = I_c$ the equilibrium point will be close to the zero current equilibrium, $\mathbf{n}_{eq}(I_c) = \mathbf{n}_{eq}(0) + \Delta\mathbf{n}$ with $\Delta\mathbf{n} \propto I_c \propto \alpha$. Expanding (7) up to linear terms in α we get an approximate stability condition

$$\omega_I \nabla \cdot \mathbf{f}_{st}|_{\mathbf{n}_{eq0}} \leq \alpha \nabla^2 \varepsilon|_{\mathbf{n}_{eq0}} \quad (8)$$

with equality achieved at the critical current. Importantly, all quantities in (8) are evaluated at the unperturbed equilibrium point $\mathbf{n}_{eq}(0)$. In comparison, using conditions (4) one needs to perform an explicit calculation of $\mathbf{n}_{eq}(I_c)$ even in the case of the first order expansion in α (e.g. Ref. 4,9). This welcome simplification stems from $\text{div}\mathbf{F}|_{I=0} \sim \alpha$ holding for any \mathbf{n} , while $\text{Tr} \hat{D}|_{I=0} \sim \alpha$ holds only at $\mathbf{n}_{eq}(0)$.

For $\boldsymbol{\tau}_{st}$ given by Eq. (6) one gets

$$\nabla \cdot \mathbf{f}_{st} = -\frac{1}{\sin\vartheta} \frac{d}{d\vartheta} (g(\cos\vartheta) \sin^2\vartheta). \quad (9)$$

where ϑ is the angle between \mathbf{s} and \mathbf{n} . Representative graphs of $\nabla \cdot \mathbf{f}_{st}(\vartheta)$ are shown in Fig.1(b) for the Slonczewski form² of $g(\vartheta)$. We observe that: (a) Divergence $\nabla \cdot \boldsymbol{\tau}_{st}$ can substantially differ from $|\boldsymbol{\tau}_{st}|$, i.e., the destabilization of noncollinear equilibria may actually require larger current. (b) The switching ability $\nabla \cdot \mathbf{f}_{st}$ vanishes at a critical angle ϑ_* (Fig.1(b)). Equation (8) predicts infinite critical current for the equilibrium points lying on the “critical circle” (CC) defined by $\vartheta(\phi, \theta) = \vartheta_*$ (more precisely, at CC the approximation (8) breaks down and I_c is just large). The critical circle divides the unit sphere into two parts. Spin-transfer torque destabilizes the energy extrema in one of them (which one – depends on the current direction), while in the other it makes them more stable. (c) The signs of I_c are opposite for equilibria located on different sides of a CC. This circumstance is especially relevant when one considers different models of $g(\vartheta)$. For example in the Slonczewski’s case ϑ_* depends on the spin polarization P and varies from $\vartheta_*(P=0) \gtrsim \pi/2$ to $\vartheta_*(P=1) = \pi$. In contrast, for a popular approximation $g = \text{const}$, one has $\vartheta_* = \pi/2$ independently of P . The difference between the models becomes crucial for an equilibrium located between the respective CC’s: a given current would have a stabilizing effect in one model, and destabilizing in another.

As an illustration, consider a typical nanopillar⁷ with an (x, y) easy plane and an easy axis $\boldsymbol{\nu} \perp \hat{z}$, so that $\varepsilon = \frac{1}{2}\omega_p(\mathbf{n}\hat{z})^2 - \frac{1}{2}\omega_a(\mathbf{n}\boldsymbol{\nu})^2 - \gamma(\mathbf{H} \cdot \mathbf{n})$. Magnetic field is in-plane perpendicular, $\mathbf{H} \perp \hat{z}$, $\mathbf{H} \perp \boldsymbol{\nu}$, and the polarizer direction is $\mathbf{s} \parallel \boldsymbol{\nu}$ (Fig. 2). In this setup the energy minima M_1 and M_2 are located at $\pm\boldsymbol{\nu}$ at $H = 0$, move towards each other with increasing H , and finally merge with the saddle point L as the field reaches the easy axis anisotropy field $H_A = \omega_a/\gamma$. The switching diagrams for

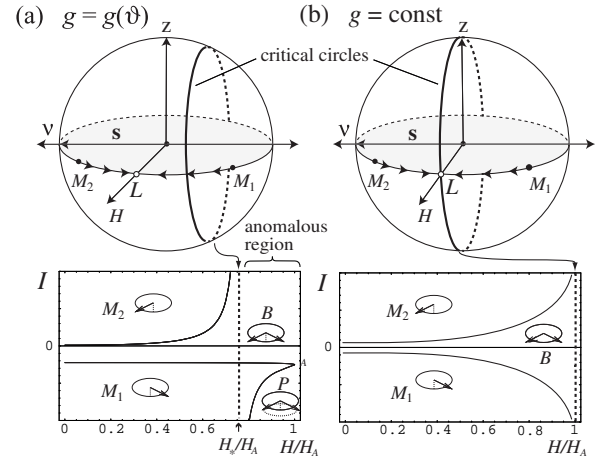


FIG. 2: Critical circles and the “anomalous” stabilization region. Upper panels: collinear device with $\mathbf{s} \parallel \boldsymbol{\nu}$ and $H \perp \hat{z}$, $H \perp \boldsymbol{\nu}$. The energy minimum points M_1 and M_2 move with increasing H as shown by the arrows. Critical circles shown for (a) generic $g(\vartheta)$ and (b) $g = \text{const}$. Lower panels: switching diagrams. In the regions M_1 and M_2 one equilibrium is stable, in B both are stable, and in P both are unstable.

a generic $g(\vartheta)$ dependence (Fig. 2a) and the special case of $g = \text{const}$ (Fig. 2b) are qualitatively different^{8,9} with the former displaying the “anomalous” region (Fig. 2a). In our approach the “anomaly” is naturally explained by the fact that the minimum point $M_1(H)$ crosses the critical circle at $H = H_*$. For $g = \text{const}$ the minima never cross the critical circle, hence the anomalous region is absent. Note that the $\tau_{st}(\vartheta)$ dependence produced by the $g = \text{const}$ approximation is qualitatively similar to the actual one. Nevertheless, it does not lead to the correct qualitative picture of switching when the equilibria of interest are close to the actual critical circle.

A similar example is provided by the nanopillars with $\mathbf{H} \parallel \boldsymbol{\nu}$ where magnetic field causes a crossing of the critical circle by an energy maximum point. That crossing naturally explains the peculiar sign change of the corresponding critical current found in Ref. 4.

Sensitivity to the $g(\theta)$ angular dependence turns out to be of crucial importance for the interpretation of the “spin-flip transistor” (a nanopillar with $\mathbf{s} \perp \hat{z}$, $\mathbf{s} \perp \boldsymbol{\nu}$) precession experiment.¹⁰ Here the calculations with $g = \text{const}$ ^{13,14} forbid precession cycles (P) at zero magnetic field, but find them in external field H antiparallel to \mathbf{s} . Based on this, Ref. 10 interpreted the observation of precession at $H = 0$ as an indication that an additional “field-like” term had to be introduced in Eq. (6). Within the framework of our analysis, the absence of P states at zero field is due to the fact that at $g = \text{const}$ the M -points stay on the critical circle (Fig. 3a) and cannot be destabilized. The antiparallel field is required to shift the M -points away from CC. However, for general $g(\vartheta)$, the M -points are away from CC even at $H = 0$ (Fig. 3b). They can be locally destabilized, producing P states by Hopf bifurcation without any field-like terms.¹² The $H = 0$ results of Refs. 13 and 14 are sensitive to the angular dependence $g(\vartheta)$ in a manner that would be hard to foresee without the notion of a critical circle.

To further demonstrate the power of the analysis based on Eqs. (8) and (9), consider experiment¹¹ performed on a nanopillar device with an unusual “wavy” $\tau_{st}(\vartheta)$ dependence (Fig. 4a). In this case there are two critical circles, CC_1 and CC_2 , defined by the angles $\vartheta_{*1,2}$. At zero external field the energy minima $M_{1,2}$ fall into the regions of

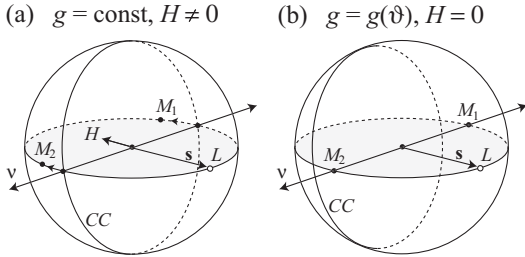


FIG. 3: Spin-flip transistor geometry. (a) For $g = \text{const}$ local destabilization of the energy minima requires external field H to shift $M_{1,2}$ away from the critical circle CC . (b) For $g = g(\vartheta)$ the minima are away from CC even at $H = 0$.

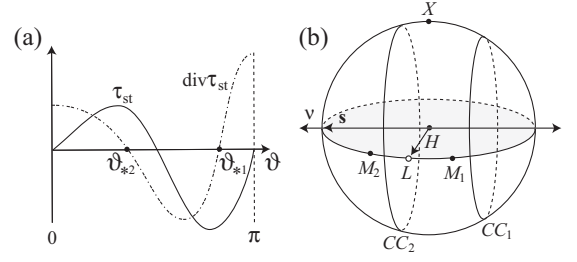


FIG. 4: (a) “Wavy” $\tau_{st}(\vartheta)$ dependence (solid line, Ref. 11) and corresponding $\nabla \cdot \tau_{st}$ (dashed line). (b) Critical circles $CC_{1,2}$ and positions of minimum points $M_{1,2}$ at an intermediate value of field H . The energy maximum point is X .

the same sign of $\nabla \cdot \tau_{st}$ and can be destabilized simultaneously, producing a precession cycle.¹¹ With increasing current, the cycle gradually approaches the energy maximum point X . Eventually spin-transfer stabilizes that point⁴ by closing the contour on it.¹¹ The notion of critical circles suggests an experiment capable of providing additional evidence for the “wavy” $\tau_{st}(\vartheta)$ dependence. If an in-plane perpendicular H is applied (Fig. 4b), the energy minima $M_{1,2}$ are shifted towards the saddle point L . As $\vartheta_{*1,2}$ are not symmetric w.r.t. $\pi/2$, there will be an interval of fields where M_1 had already crossed CC_1 and moved into the middle region, while M_2 remains in the left region. In this interval $\nabla \cdot \tau_{st}$ has opposite signs for $M_{1,2}$ and normal switching between M_1 and M_2 will be possible. Further increase of H will put both M -points into the middle region, where they will be again destabilized by the same current direction. However, in contrast with the $H = 0$ case, now the same current direction will also destabilize X , so the P state evolution will be different.¹²

Let us now turn to stabilization of the saddle points. Here $\det \hat{D}_{I=0} < 0$, so the process requires a change of

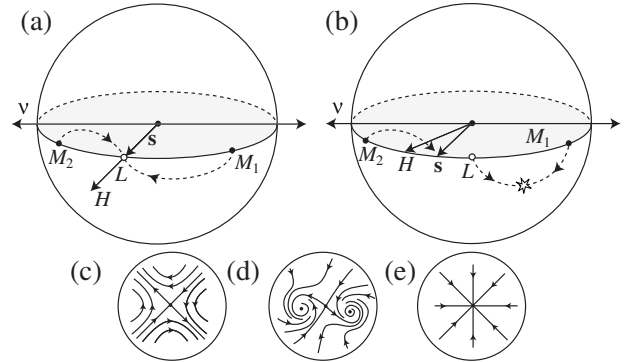


FIG. 5: (a) Spin-flip transistor: $\mathbf{s} \perp \hat{z}$, $\mathbf{s} \perp \boldsymbol{\nu}$, $\mathbf{H} \parallel \mathbf{s}$. The dashed lines show how the positions of the equilibria M_1 and M_2 change with increasing current and merge with the saddle L . (b) General in-plane directions of \mathbf{s} and \mathbf{H} . The saddle merges with one of the minima, while the other one asymptotically approaches \mathbf{s} . (c-e) transformation of the field \mathbf{F} during the merging of a saddle with two foci in case (a).

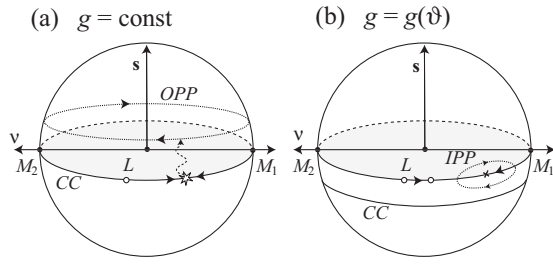


FIG. 6: “Magnetic fan” geometry. (a) At $g = \text{const}$ the point M stays on CC until it collides with L , creating a large “OPP cycle” (dotted line). (b) At $g = g(\vartheta)$ M is away from CC . Its local destabilization can create a small “IPP cycle”.

sign of $\det \hat{D}$. An example is provided by a spin-flip transistor where the spin torque attracts \mathbf{n} to the saddle point and eventually stabilizes L .^{13,14} Notably, stabilization is always accompanied by a simultaneous discontinuous change in the nature of other equilibria. At $H = 0$ the M -points lose their stability just as L becomes stable.¹³ With the field parallel to \mathbf{s} (note the difference with the antiparallel case discussed above) the current leads to a significant deviation of the M -points from their initial positions (Fig. 5(a)). At the critical current, $M_{1,2}$ approach L and merge with it, forming a stable center. We start by explaining why those simultaneous transformations are not a coincidence. The saddle point is stabilized by becoming a stable center. As topological defects of the vector field \mathbf{F} , saddles and centers differ in the winding number¹⁵ which is a topological characteristic equal to $n = -1$ for a saddle and $n = 1$ for a center or focus. Since the total winding number is conserved (the Poincaré index theorem), a saddle point cannot be transformed into a center locally. The saddle-to-center transformation has to either proceed via merging with other defects (Fig. 5(c-e)), or be accompanied by a simultaneous change of nature of the far away equilibria.

More insight comes from considering a generic case of \mathbf{H} and \mathbf{s} pointing in arbitrary in-plane directions (Fig. 5(b)). Here L merges with one of the minima annihilating both equilibria, while the other minimum approaches \mathbf{s} . Such merging is allowed by the winding number conservation and in fact the bifurcation theory⁶ shows that it is the most general case of the *saddle-node bifurcation*; i.e., the saddle point is normally not stabilized but rather destroyed in a collision with an energy extremum point. Stabilization happens only in special

circumstances, such as \mathbf{s} pointing exactly into L . In this case L remains an equilibrium for the arbitrarily large current and cannot disappear. That restriction produces the *transcritical bifurcation*⁶ where the energy extremum and the saddle exchange their nature in a collision. We find the critical current to be

$$\omega_I = \frac{\sqrt{-\det \hat{D}|_{I=0, \alpha=0}}}{g(0)}. \quad (10)$$

The above formula remains a good estimate in the case of a small misalignment between \mathbf{s} and L . It also works for the spin flip transistor (Fig. 5a) even though here additional symmetries produce a more rare *fork bifurcation*.

To sum up, the saddle point stabilization is associated with a merging or a close approach of equilibria, and thus can be detected without even calculating the dynamic matrix. A non-local bifurcation can only occur in devices of exceptionally high symmetry.

Local destabilization and equilibrium merging are two alternative switching mechanisms which can compete with each other. Consider the $\mathbf{s}||\hat{\mathbf{z}}$ “magnetic fan” experiment¹⁶ (Fig. 6). Here the $g = \text{const}$ approximation is special since the critical circle goes through the M -points. It predicts a merging of L and M_1 , after which the system jumps into an “OPP cycle” (Fig. 6a). For angle-dependent $g(\vartheta)$ the CC is away from the M -points, allowing for a competing scenario with local destabilization of M_1 producing an “IPP cycle” (Fig. 6b).¹² We estimate the critical currents as $\omega_{I(IPP)} \approx \alpha \omega_p / g'(\pi/2)$ and $\omega_{I(OPP)} \approx \omega_a / g(\pi/2)$. Using Slonczewski’s g and experimental parameters¹⁶ we find $\omega_{I(OPP)} / \omega_{I(IPP)} \approx 0.2$, which yields an OPP cycle scenario in accord with experiment. Furthermore, we predict that a device with a sufficiently large ω_a would manifest an IPP cycle.

To conclude, we found that the ability of electric current to destabilize magnetization at its energy minimum (or to force it to be stable at its energy maximum) is determined by the spin torque divergence. We also showed that the sphere swept by the magnetization vector is divided into stabilization and destabilization regions by critical circles. Finally, we demonstrated that saddle points are stabilized via a topologically distinct route of merging with other equilibria, and discussed the competition between such a merging and local destabilization.

It is our pleasure to thank S. Garzon, R. A. Webb, and R. R. Ramazashvili for stimulating discussions.

* sodemann@physics.sc.edu, yar@physics.sc.edu

¹ L. Berger, J. Appl. Phys. **49**, 2156 (1978); Phys. Rev. B **33**, 1572 (1986); Phys. Rev. B **54**, 9353 (1996).

² J. C. Slonczewski, J. Magn. Magn. Mater. **159**, L1 (1996).

³ D. C. Ralph and M. D. Stiles, J. Magn. Magn. Mat. **320**, 1190 (2008).

⁴ Ya. B. Bazaliy, B. A. Jones, and S. C. Zhang, Phys. Rev.

B **69**, 094421 (2004).

⁵ C. Serpico, J. Magn. Magn. Mat. **290-291**, 48 (2005); R. Bonin, C. Serpico, G. Bertotti, I. D. Mayergoyz, and M. d’Aquino, Eur. Phys. J. B **59**, 435 (2007).

⁶ J. D. Crawford, Rev. Mod. Phys. **63**, 991 (1991).

⁷ J. A. Katine, F. J. Albert, R. A. Buhrman, E. B. Myers, and D. C. Ralph, Phys. Rev. Lett. **84**, 3149 (2000).

- ⁸ N. Smith, J. A. Katine, J. R. Childress, and M. J. Carey, IEEE Trans. Magn. **41**, 2935 (2005), *ibid.* **42**, 114 (2006).
- ⁹ I. Sodemann and Ya. B. Bazaliy, J. Appl. Phys. **105**, 07D114 (2009).
- ¹⁰ T. Devolder, A. Meftah, K. Ito, J. A. Katine, P. Crozat, and C. Chappert, J. Appl. Phys. **101**, 063916 (2007).
- ¹¹ O. Boulle, V. Cros, J. Grollier, L. G. Pereira, C. Deranlot, F. Petroff, G. Faini, J. Barnaś, and A. Fert, Nat. Phys. **3**, 492 (2007).
- ¹² We have confirmed these qualitative predictions numerically.
- ¹³ X. Wang, G. E. W. Bauer, and T. Ono, Jap. Jour. Appl. Phys. **45**, 3863 (2006).
- ¹⁴ H. Morise and S. Nakamura, Phys. Rev. B **71**, 014439 (2005).
- ¹⁵ N. D. Mermin, Rev. Mod. Phys. **51**, 591 (1979).
- ¹⁶ D. Houssameddine, U. Ebels, B. Delaet, B. Rodmacq, I. Firastrau, F. Ponthenier, M. Brunet, C. Thirion, J.-P. Michel, L. Prejbeanu-Buda, M.-C. Cyrille, O. Redon and B. Dieny, Nat. Mater. **6**, 447 (2007).